# Extraction of Five Photovoltaic Parameters of Nature-based Dye-Sensitized Solar Cells using Single Diode Model

S. Ezike[1*], B. J. Yerima[2], W. Dunama[3], A. Babangida[4], A. D. Ahmed[2]

1. Modibbo Adama University, Yola, Adamawa State, Nigeria.
2. Department of Physics, Faculty of Physical Sciences, Modibbo Adama University, Yola, Adamawa State, Nigeria.
3. Department of Mathematics, Faculty of Physical Sciences, Modibbo Adama University, Yola, Adamawa State, Nigeria.
4. Department of Physics, Aminu Saleh College of Education Azare, Bauchi State, Nigeria.

## Abstract

Dye-sensitized solar cells (DSSCs) are among the family of third generation photovoltaic (PV). DSSCs are promising with the theoretical predicted value for power conversion efficiency (PCE) of 20%. In this work, explicit equations for the single-diode equivalent circuit model parameters of a solar cell are modeled based on the characteristic points on the I-V curves that do not require the short-circuit and open-circuit slopes as the input data. The equations are used to calculate the five model parameters (n, $R_s$, $R_{sh}$, $I_{ph}$, $I_o$) of a standard solar cell-based DSSC composed of different natural photosensitizers. The results obtained show that four (~28.5%) devices with natural photosensitizers (bitter gourd, sun flower, rose flower, tomato) manifest the parameter irregularities, i.e. they have negative series resistance or complex shunt resistance. Despite the occurrence of irregular parameters, there is still a good match between the calculated and measured photoelectric characteristics. This supports the idea that the nature of the parameter values does not matter provided that there is a good match between the measured and calculated I-V characteristics. The bitter gourd-based DSSC demonstrates the most promising photosensitizer for DSSC fabrication based on the values of the parameters. Hence, the agreement of the calculated and measured parmeters suggests that modeling is a good approach for extraction the solar parameters.

**Keywords:** *Natural photo-sensitizers, Dye-sensitized solar cells, Irregular parameters, Explicit equations, Single-diode model.*

## 1. Introduction

For past several decades, research in the field of photovoltaic (PV) has progressed from the first generation solar cell to the third generation solar cell. Therefore, the interest in renewable energy resources has increased, and in this case, the PV systems are more attractive [1-5]. The model of a PV device usually made up of an equivalent circuit and a set of parameters that depicts its electrical response and operation. The calculation of these parameters is not a common process as they are not available in PV module's datasheet, and their values vary with the operating conditions [6]. Several research works have been carried out in the recent times on the extraction of the PV model parameters and the previous works presenting numerous methods of different nature, reliability, complexity, and the required input data. These methods are usually referred to as the numerical, the non-iterative, and the optimization approaches. The numerical or iterative methods

deal with a system of few equations that is solved numerically [7-11], in a trivial-and-error manner or via another iterative algorithm [12-15]. The equations are usually obtained by applying the PV model equation to specific conditions such as short-circuit (SC), open-circuit (OC) or maximum power point (MPP). This method gives generally a high accuracy but undergoes initialization and convergence problems, high calculation cost, and solution less than optimal [6, 16-18]. The non-iterative or explicit or direct methods use a set of equations as well but are solved symbolically/explicitly without iterations resulting in easier formulation and application [17, 19-24]. These approaches are essentially variations of the numerical method that use a series of simplifications and empirical observations to get an explicit formulation. Quite often, they are employed in the initialization step of the numerical methods [22].

The non-iterative methods are easier to carry out and more computationally efficient but give a lower accuracy [18], although some of these approaches perform quite appropriately [25]. The optimization or artificial intelligence or iterative or curve-fitting or soft-computing methods follow a non-technologically scientific approach, where the model equation is optimally fitted on a set of measurements usually from I-V curves. Different evolution reported [26] and curve fitting [27] algorithms are available. This method reveals generally a high accuracy and near-global optimally but prone to computational complications and difficulties in the method's parameter adjustment.

Furthermore, another significant aspect of a parameter extraction technique is the required input data. In some cases, the datasheet information furnishes, for example, SC, OC, and MPP, and temperature coefficients [17, 19], while others require additional operating points or/and the gradient of the I-V curve at SC or OC [20]. Generally, the former cases are preferable as they can be applied more easily and universally not necessitating extra measurement [23, 28]. Moreover, there is presently an argument in the literature on whether the extracted parameters should be limited to real positive numbers to have a physical meaning [9, 22] or should be allowed to take negative or complex values referred to as parameter irregularities if the resulting curve better matches the measurements [19, 25]. In addition, other desirable qualities of such a method are to be accurate, straightforward, computationally efficient, and applicable to different PV technologies [6, 23].

Recently, fourteen natural dyes (photosensitizers) have been found efficient enhancing photo-absorbers using some standard selection and grading criteria [29]. Furthermore, the study of the energy bandgap of these dyes confirms that they are good photosensitizers for an efficient DSSC production [30]. It is against this background, in this paper, we developed an explicit 1-diode/2-resistors equivalent circuit model equation independent from slope measurement from previous works [19, 20, 22] to determine the five photovoltaic parameters of the fourteen DSSCs from different locally produced natural dyes (light absorbers).

## 2. Materials methods

### 2.1. Mathematical formulation of single-diode PV model

The single-diode model is the record of the description of the theory of the first PV model, developed initially for single-crystalline silicon PV cells but it remains to this day the most popularly applied one owing to its simplicity [7, 31]. Many more complicated models consider two or three diodes for enhanced accuracy at low irradiance, and often times extra voltage-dependent current sources to explain the unstable operation or the recombination occurrence in some thin film technologies [32]. This paper is limited to the single-diode model, as this is the PV model on which most of the non-iterative parameter extraction approaches are based, and evaluates its usefulness on all commercial PV technologies, single/multi-crystalline silicon, and thin-film.

The model is made up of an equivalent circuit depicted in figure 1 and a set of five parameters $(I_{ph}, I_o, a/n, R_s, R_{sh})$: the photocurrent $I_{ph}$, the diode saturation current $I_o$, the diode ideality factor n (or its modified version, a), the series resistance $R_s$, and the shunt resistance $R_{sh}$.
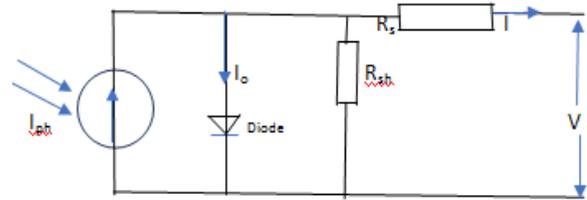


**Figure 1 Electrical equivalent circuit of the single-diode solar cell [33]**

Most of the times, the modified is usually written in the literature as in equation (1).

$$a = N_s n V_T \tag{1}$$

where $N_s$ is the number of series-connected cells, n the diode factor, and $V_T$ is the thermal voltage given (Equation (2)) using [34].

$$V_T = \frac{kT}{q} \tag{2}$$

where $k = 1.381 \times 10^{-23}\ JK^{-1}$ is the Boltzmann constant, $T = 300\ K$ is the temperature in Kelvin, and $q = 1.602 \times 10^{-19}\ C$ is the electron charge. The five model parameters depend on both the nature of the PV modules and the working conditions, namely incidence irradiance and cell temperature. The irradiance is usually observed to change proportionally to $I_{ph}$, and $R_{sh}$ in an inversely proportional manner; the temperature effect is generally considered to be insignificant and linear in $I_{ph}$, strong and exponential in $I_o$, and strong and directly proportional in n. The dependence of $R_s$ is not yet clear; some studies

consider it to remain constant [35] and others suggest that it depends on both irradiance and temperature [22]. Normally, the five parameters are not considered to be altered by the operating point, i.e. they do not vary along the I-V curve. For some technologies, however, it has been reported to change with the current, especially the diode factor and series resistance; here, the former approach is considered, which is adopted by all the parameter extraction methods studied. It is worth noting that sometimes the literature neglects one or both resistances for simplicity [36].

The current-voltage equation is given implicitly by equation (3) [37, 38].

$$I = I_{ph} - I_o \left( e^{\frac{V + IR_s}{a}} - 1 \right) - \frac{V + IR_s}{R_{sh}} \tag{3}$$

This equation cannot be solved explicitly, and requires a numerical solution, which leads to some difficulties during the computation. On the other hand, an equivalent explicit formulation has appeared lately in the literature, employing the principal branch of the Lambert W function $W_0$ from equations (4) and (5) [39].

$$I = \frac{R_{sh}(I_{ph} + I_s) - V}{R_{sh} + R_s} - \frac{a}{R_s} W_o \left( \frac{R_{sh}R_sI_o}{aV_T(R_{sh}+R_s)} e^{\left( \frac{R_{sh}R_s(I_{ph}+I_s)+VR_{sh}}{a(R_{sh}+R_s)} \right)} \right) \tag{4}$$

$$V = R_{sh}(I_{ph} + I_s) - (R_s + R_{sh}) - aW_o \left\{ \frac{R_{sh}I_s}{a} e^{R_{sh}\left( \frac{I_{ph}+I_s-I}{a} \right)} \right\} \tag{5}$$

One can directly find the current for a given value of voltage using equation (4) or the voltage via equation (5), which makes the computation easy and robust, in contrast to equation (3). The Lambert W function is readily available in all the calculation procedures [37].

It is worth noting that the power is obtained by the product of V and I at different loads. The I-V graph can be plotted, and the peak of the graph corresponds to maximum power, which is represented in equation (6) [40, 41].

$$P_{max} = V_{max}I_{max} \tag{6}$$

The fill factor (FF) of a cell is essentially a measure of the quality of the solar cell; it is the ratio of maximum power output referring to equation (6) to the product of the open-circuit voltage, and short circuit current is expressed in equation (7) [42, 43].

$$FF = \frac{V_{max}I_{max}}{V_{oc}I_{sc}} \tag{7}$$

The conversion efficiency of a cell that determines utmost the reliability of the cell is defined as the ratio of electrical energy output to the light energy input, which is represented in equation (8) [44, 45].

$$\eta = \frac{V_{mp}I_{mp}}{P_i A} \times 100 \ \% \tag{8}$$

where $P_i$=1000 is the identical optical power in watts/m$^2$at average solar spectrum at AM 1.5 and A is the illuminated area in cm$^2$.

## 2.2. Non-iterative parameter extraction method

In this work, a combination of different non-iterative methods available for the parameter extraction of the single-diode PV module is adopted assuming $R_{sho} = R_{sh}$ to avoid measuring the SC slope of the I-V curve. The combination of the three non-iterative methods adopted is as follows: first, the modified factor a (or the shape factor n) and $I_{ph}$ are adopted via the Sera's equation [19], and then $R_s$ and $R_{sh}$ via the Hejri's equation [22], and finally, $I_0$ via the Khan's equation [20] such that the five parameters are found via equations (9) to (13).

$$a = \frac{2V_{mp} - V_{oc}}{\ln\left(\frac{I_{sc} - I_{mp}}{I_{sc}}\right) + \frac{I_{mp}}{I_{sc} - I_{mp}}} \quad \text{or} \quad n = aV_T \tag{9}$$

$$R_s = \frac{V_{mp}}{I_{mp}} - \frac{\left(\frac{2V_{mp} - V_{oc}}{I_{sc} - I_{mp}}\right)}{\ln\left(\frac{I_{sc} - I_{mp}}{I_{sc}}\right) + \frac{I_{mp}}{I_{sc} - I_{mp}}} \tag{10}$$

$$R_{sh} = \left( \frac{R_s}{\frac{I_{sc}}{a}e^{\left(\frac{R_sI_{sc}-V_{oc}}{a}\right)}} \right)^{\frac{1}{2}} \tag{11}$$

$$I_{ph} = I_{sc} \tag{12}$$

$$I_o = I_{sc}e^{\frac{-V_{oc}}{a}} \tag{13}$$

The equations are employed to calculate the required five photovoltaic parameters (a/n, $R_s$, $R_{sh}$, $I_{ph}$, $I_0$) for fourteen DSSCs devices-based different locally produced natural photo-absorbers.
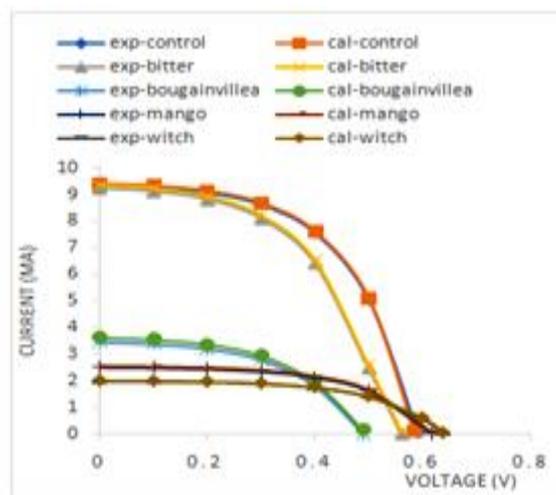
In case the negative series resistance problem occurs, it means that the solar cell has a very small resistance. Equation (10) can result in an unrealistic negative value due to the natural logarithm term in the denominator. In this case, the initial value of $R_s$ can be set to zero, and one can use the slope of the line connecting the SC and MPPs on the I-V curve as an estimation of $R_{sh}$ given by equation (14) [22].

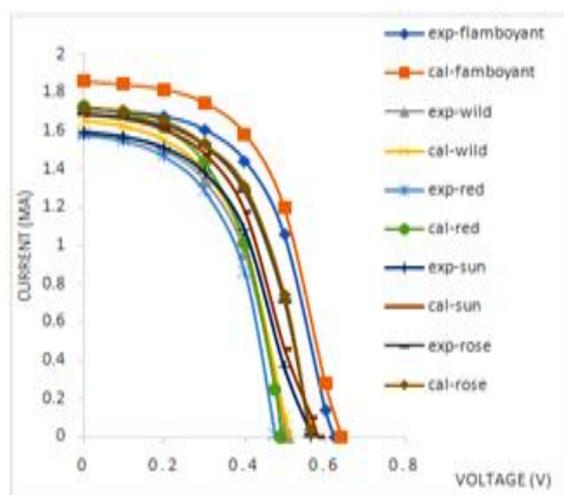$$R_{sh} = \frac{V_{mp}}{I_{sc} - I_{mp}} \qquad (14)$$

## 3. Results and discussion

The measured I-V data of one synthetic DSSC and fourteen nature-based DSSCs consisting of different natural dyes/photo-absorbers is reported in this work. Figures 2 (a-c) depict the I-V curves showing the photovoltaic cell is at a constant current source for low voltages with a current approximately equal to $I_{sc}$. With increasing voltage at a certain point, the current begins to drop off exponentially to zero at $V_{oc}$. The system design is to operate the cell at maximum power point, MPP ($V_{mp}$, $I_{mp}$). However, the system design is complicated by the fact that the maximum power point varies with irradiance and temperature [46].
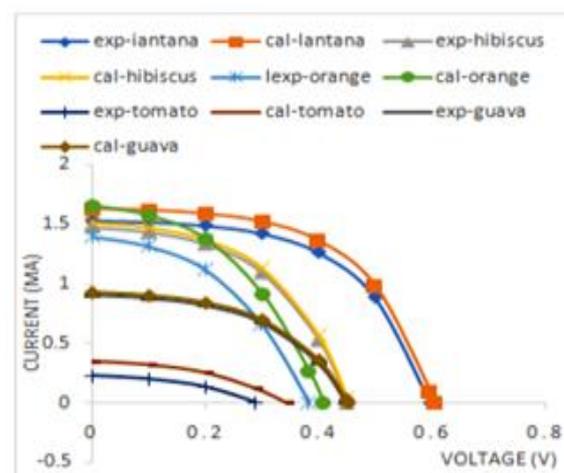
Each of the fabricated DSSC has an effective area (1 cm$^2$) of exposure to light. Using the maximum power point from I-V curve, $P_i$ = 1000 watts/m$^2$, and the effective area (1 cm$^2$) of DSSC, the $P_{max}$, FF, and η% were calculated (Table 1) using equations (6), (7), and (8), respectively. The values of $P_{max}$, FF, and η lie in the ranges 0.027-3.028 mW, 0.35-0.76, and 0.03-3.02%, respectively. The results show that among the DSSC based on bitter gourd has the highest conversion efficiency of 2.57% next to that of the standard with 3.02% while, DSSC based on tomato has the least 0.03%. The synthetic-based DSSC has the highest η compared with nature-based DSSCs [47]. Also the synthetic-based DSSC has the highest $I_{sc}$ among all the cells. Among the nature-based DSSSCs, bitter gourd-based DSSC has the best $I_{sc}$ and η corresponding to 9.244 mA and 2.57%, respectively. Bougainvillea-based DSSC has a better $I_{sc}$ than Mango peel-based DSSC; however, η of Mango peel-based DSSC is higher than that of Bougainvillea-based DSSC. The relatively higher performance of Bitter gourd-based DSSC over other nature-based DSSCs could be due to narrow energy band gap of the active material and good energy level offset between the semi-conductor and dyes [41]. The narrow energy band gap enhances excitation of charge carrier (electrons) from highest occupied mobile orbital (HOMO) to lowest unoccupied mobile orbital (LUMO). Good energy level offset between the semi-conductor and dyes enhances collection of electrons.
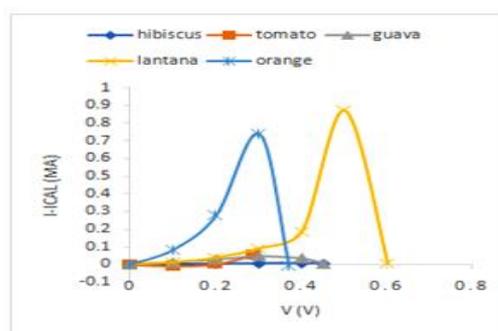


(a)



(b)



(c)

**Figure 2: I-V curve fitting of calculated and experimental data for (a) control, witch seed flower, mango, bitter gourd and bougainvillea, (b) flamboyant, red cockscomb, rose, wild marigold, and sun flower, (c) hibiscus, lantana, orange, tomato and guava.**

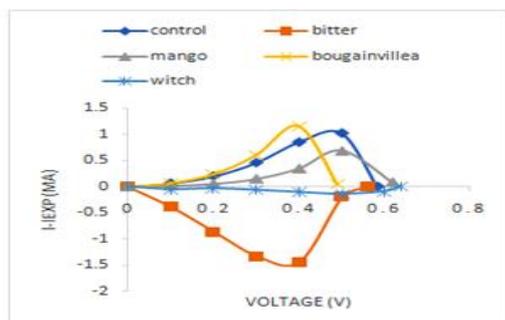**Table 1: Characteristic point of DSSCs for various photosensitizers**

| Source of natural dye | | Photovoltaic parameters | | | | | | |
|---|---|---|---|---|---|---|---|---|
| English Name | Scientific Name | $I_{sc}$ (mA) | $I_{mp}$ (mA) | $V_{mp}$ (V) | $V_{oc}$ (V) | $P_{max}$ (mW) | FF | η % |
| Control | TiO₂/N719 | 9.355 | 7.574 | 0.4 | 0.590 | 3.028 | 0.54 | 3.02 |
| Witch seed flower | Striga hermonthica | 1.970 | 1.379 | 0.4 | 0.639 | 0.551 | 0.43 | 0.55 |
| Bitter gourd | Momordica charantia | 9.244 | 6.450 | 0.4 | 0.536 | 2.580 | 0.51 | 2.57 |
| Bougainvillea | Bougainvillea | 3.450 | 2.783 | 0.3 | 0.484 | 0.834 | 0.50 | 0.83 |
| Flamboyant | Delonix regia | 1.717 | 1.442 | 0.4 | 0.610 | 0.576 | 0.55 | 0.57 |
| Wild marigold | Calendula arvensis | 1.600 | 0.957 | 0.3 | 0.504 | 0.287 | 0.35 | 0.28 |
| Red cockscomb | Celosia cristata | 1.580 | 1.290 | 0.3 | 0.490 | 0.387 | 0.49 | 0.38 |
| Lantana | Lantana camera | 1.530 | 1.262 | 0.4 | 0.600 | 0.504 | 0.54 | 0.50 |
| Hibiscus | Hibiscus rosa sinensis | 1.480 | 1.090 | 0.3 | 0.450 | 0.327 | 0.49 | 0.32 |
| Sun flower | Helianthus | 1.590 | 1.081 | 0.4 | 0.530 | 0.432 | 0.51 | 0.43 |
| Rose flower | Rosa | 1.690 | 1.283 | 0.4 | 0.563 | 0.512 | 0.53 | 0.51 |
| Orange peel | Citrus aurantium | 1.400 | 1.121 | 0.2 | 0.370 | 0.224 | 0.43 | 0.22 |
| Tomato | Lycopersicon esculentum | 0.230 | 0.135 | 0.2 | 0.290 | 0.027 | 0.40 | 0.03 |
| Mango peel | Mongifera indica | 2.51 | 2.130 | 0.4 | 0.618 | 0.852 | 0.76 | 1.00 |
| Guava peel | Psidium guajava | 0.900 | 0.669 | 0.3 | 0.452 | 0.201 | 0.49 | 0.20 |

The performance metrics of fourteen different nature-based DSSCs were obtained using RMSE. Figure 3 shows the RMSE, which measures the extent the calculated values deviate from the experimental values. RMSE is a good measure of how accurately a model predicts a response. It decides the overall quality of prediction. The performances of bitter gourd, rose, and sun flower-based DSSCs show that the cells have negative calculated current values unlike other dyes-based DSSCs. The smallest RMSE value indicates better fit [48]. Hence, it is worth noting that sometimes it is possible to differentiate the explicit calculated data that gives the most approximation to the measured data but it is not possible to choose the best option with a proper criterion beyond a visual impression.
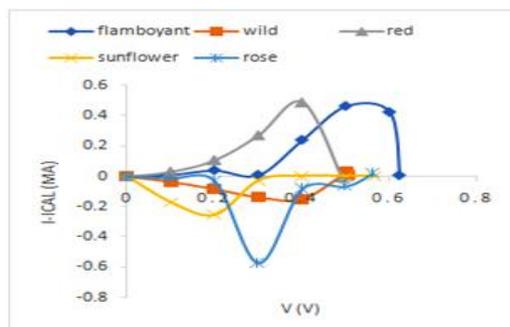


**(a)**



**(b)**



**(c)**

**Figure 3: I-V curve fitting of corresponding root mean square error (RMSE) for (a) control, witch seed flower, mango, bitter gourd and bougainvillea, (b) flamboyant, red cockscomb, rose, wild marigold, and sun flower, (c) hibiscus, lantana, orange, tomato and guava.**

For this reason, the results in figure 3 have been analyzed using the percentage normalized RMSE given by equation (15).

$$\varepsilon = \frac{1}{I_{sc}} \sum_{j=1}^{N} \left(I_{cal,j} - I_{exp,j}\right)^2 \times 100\ \% \qquad (15)$$

Figure 4 depicts the RMSE of the different solar cells studied. Among the nature-based DSSCs, hibiscus flower-based DSSC has the least percentage value (2.23%) of RMSE unlike orange-based DSSC with the highest value (25.95%) of RMSE. Bitter gourd-based DSSC possessing the highest η has the RMSE value of 8.91%. The synthetic-based DSSC has RMSE value of 5.73%. The results suggest that the experimental values and calculated values of nature-based DSSC deviate in increasing order of: $hibiscus \rightarrow rose \rightarrow mango \rightarrow witch \rightarrow wild \rightarrow guava \rightarrow bittergourd \rightarrow latana \rightarrow helianthus \rightarrow tomato \rightarrow flamboyant \rightarrow red \rightarrow boungainvillea \rightarrow ornage$. The results

show that hibiscus-based DSSC has the least deviation, while orange-based DSSC has the highest deviation. It shows that there is data agreement between the experimental data and calculated data, which could be confirmed from figure 2.

In table 2, the values of the photovoltaic parameters $R_{sh}$, $R_s$, a/n, $I_s$, and $I_{ph}$ have been determined from the method we have developed. This method has been applied to fourteen DSSCs fabricated by our group in a Laboratory at Bangalore College of Engineering Bangalore, India to determine these photovoltaic parameters using equation (1) and equations (9) to (14). The validity of the assumptions herein has been reported elsewhere [19, 22, 24]. The results show no execution failure and only four ($\sim$28.5%) irregular parameters (negative series resistances/complex shunt resistances) belonging to DSSCs with bitter gourd, sun flower, rose flower, and tomato photosensitizers. This indicates that the robustness of our technique is assessed through the number of irregularities found in the parameters and the failure to produce an acceptable I-V curve with the extracted parameters.
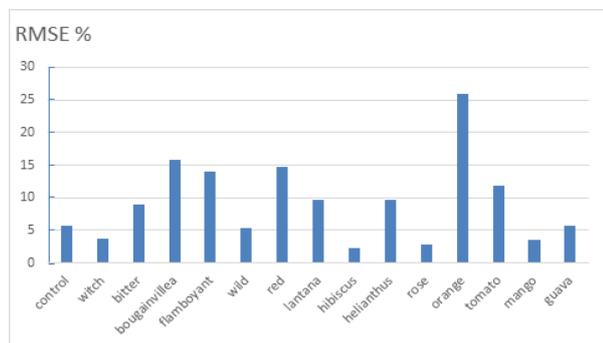


**Figure 4: RMSE of various DSSCs with different photosensitizers**

Presently, there is generally no accepted norm in the literature on whether the PV model parameters should be restricted to real positive numbers or should be allowed to get negative or complex values. There are some previous works that support the positive approach to get parameters with physical meaning [9, 22], whereas others do not adhere to this restriction if this leads to better results [19, 25]. It is worth noting that in this work, the complex values come from a negative argument in square root or logarithmic functions in equations (10) and (11). However, these irregularities were removed using equation (14) by setting $R_s = 0$ given $R_{sh}$ real values (asterisked in brackets) (Table 2), which can be used as the initial values in numerical method for better results. In general, the methods that require performing calculations on the I-V curve measurements such as extraction of the SC slope or locating a specific point carry extra computational burden.

In table 2, the modified ideality factor or shape factor, a, has all values less than unity in the range $0.01248 \leq a \leq 0.27419$, whereas the diode ideality factor, n, lies in the range $0.5 \leq n \leq 10.6$. The results reveal that DSSCs with $n > 5$ except witch seed flower and wild marigold, are those that depict irregular series resistances and corresponding complex shunt resistances. Thus this study shows that the values of a/n, $I_0$, and $R_s$ are not constant but vary along the I-V curve.

Good and efficient device always have low $R_s$ value, while the $R_{sh}$ values are should be high. Very high values of $R_s$ and very low values of $R_{sh}$ reduce $J_{sc}$ and $V_{oc}$, respectively [49]. The most efficient device (bitter gourd) among the nature-based DSSCs has the least value of $R_s$.

**Table 2 Parameters of 1-diode/2-resistors circuit equivalent model of DSSCs for various dye-photosensitizers.**

| Natural dye source | PV model parameters | | | | | | RMSE |
|---|---|---|---|---|---|---|---|
| English Name | a | n | $R_s$ ($\Omega$) | $R_{sh}$ ($\Omega$) | $I_{ph}$ (mA) | $I_o$(A) | ($\varepsilon$ %) |
| Control | 0.08096 | 3.1 | 7.4 | 199.5 | 9.355 | $6.3976\times10^{-6}$ | 5.73 |
| Witch seed flower | 0.14256 | 5.5 | 48.8 | 399.0 | 1.970 | $22.2740\times10^{-6}$ | 3.71 |
| Bitter gourd | 0.24007 | 9.3 | **-2.3**(0*) | **117.7i**(142.3*) | 9.244 | $991.2790\times10^{-6}$ | 8.91 |
| Bougainvillea | 0.04587 | 1.8 | 39.0 | 1026.7 | 3.450 | $0.0902\times10^{-6}$ | 15.79 |
| Flamboyant | 0.05569 | 2.2 | 74.9 | 3715.0 | 1.717 | $0.0300\times10^{-6}$ | 14.05 |
| Wild marigold | 0.16646 | 6.4 | 54.6 | 263.5 | 1.600 | $77.4761\times10^{-6}$ | 5.33 |
| Red cockscomb | 0.03996 | 1.5 | 94.8 | 3458.9 | 1.580 | $0.0075\times10^{-6}$ | 14.79 |
| Lantana | 0.06741 | 2.6 | 65.4 | 2188.8 | 1.530 | $0.2085\times10^{-6}$ | 9.66 |
| Hibiscus | 0.10265 | 4.0 | 12.0 | 237.0 | 1.480 | $18.4697\times10^{-6}$ | 2.23 |
| Sun flower | 0.27419 | 10.6 | **-168.6**(0*) | **731.0i**(785.8*) | 1.590 | $230.0970\times10^{-6}$ | 9.59 |
| Rose flower | 0.13710 | 5.3 | **-25.1**(0*) | **410.3i**(982.8*) | 1.690 | $27.8267\times10^{-6}$ | 2.77 |
| Orange peel | 0.01248 | 0.5 | 133.7 | 52528.9 | 1.400 | **$1.8397\times10^{-16}$** | **25.95** |
| Tomato | 0.20490 | 7.9 | **-675.3**(0*) | **2299.4i** (2105.2*) | 0.230 | $55.8543\times10^{-6}$ | 11.80 |
| Mango peel | 0.04896 | 1.89 | 58.9 | 4121.3 | 1.480 | $0.0083\times10^{-6}$ | 3.53 |
| Guava peel | 0.09635 | 3.7 | 31.3 | 522.4 | 0.900 | $8.2563\times10^{-6}$ | 5.73 |

*imaginary values

## 4. Conclusion

This work revealed that five model parameters (n, $R_s$, $R_{sh}$, $I_{ph}$, $I_o$) of DSSCs-based nature sensitizers had real values except four of the DSSCs consisting of photosensitizers: bitter gourd, sun flower, rose flower, and tomato have parameter irregularities. Despite the presence of the parameter irregularities, there is a good match between the calculated modeled data and the experimental data I-V characteristics (short-circuit, maximum point, and open-circuit) using the RMSE (ε). This implies that the irregular parameters are not necessarily an undesirable features for some applications. The results suggest that the experimental values and calculated values of nature-based DSSC deviate in increasing order of: $hibiscus \rightarrow rose \rightarrow mango \rightarrow witch \rightarrow$ $wild \rightarrow guava \rightarrow bittergourd \rightarrow latana \rightarrow$ $helianthus \rightarrow tomato \rightarrow flamboyant \rightarrow$ $red \rightarrow boungainvillea \rightarrow ornage$. Bitter gourd-based DSSC possessing the highest η has the RMSE value of 8.91%. The modified ideality factor, a, has all values less than unity in the range $0.01248 \leq a \leq 0.27419$, whereas the diode ideality factor, n, lies in the range $0.5 \leq n \leq 10.6$. The results reveal that DSSCs with $n > 5$ except witch seed flower and wild marigold are those that depict irregular series resistances and corresponding complex shunt resistance.

Therefore, five model parameters are deduced using the modeling technique, and the experimental values correspond with the calculated value despite the parameters irregularities. Hence, the parameters of bitter gourd indicate its most promising sensitizer for DSSC fabrication with $I_{sc}$ and η corresponding to 9.244 mA and 2.57%, respectively.

## 5. Acknowledgment

## 6. Conflicts of interest

The authors declare that they have no conflict of interest.

## 7. Abbreviations and symbols

| | |
|---|---|
| DSSC | Dye-sensitized solar cell |
| PV | Photovoltaic |
| PCE | Power conversion efficiency |
| RMSE | Root mean square error |
| I-V | Current-Voltage |
| SC | Short circuit |
| OC | Open circuit |
| MPP | Maximum power point |
| $I_{ph}$ | Photocurrent |
| $I_0$ | Diode saturation current |
| $n$ | Ideality factor |
| $R_s$ | Series resistance |
| $R_{sh}$ | Shunt resistance |
| $N_s$ | Number of series connected cells |
| $V_T$ | Thermal voltage |
| $k$ | Boltzmann constant |
| $T$ | Temperature |
| $q$ | Electron charge |
| $W_0$ | Lambert W function |
| $P_{max}$ | Maximum power |
| $I_{max}$ | Maximum current |
| $V_{max}$ | Maximum voltage |
| FF | Fill factor |
| $V_{oc}$ | Open-circuit voltage |
| $I_{sc}$ | Short circuit current |
| η | Efficiency |
| $V_{mp}$ | Maximum power voltage |
| $I_{mp}$ | Maximum power current |
| $P_i$ | Incident power |
| $A$ | Area |

## 8. References

[1] S.C. Ezike, A.B. Alabi, A.N. Ossai, and A.O. Aina, "Effect of tertiary butylpyridine in stability of methylammonium lead iodide perovskite thin films", Bull. Mater. Sci. Vol. 43, pp. 40, 2020, https://doi.org/10.1007/s12034-019-2002-2.

[2] S.C. Ezike, A.B. Alabi, A.N. Ossai, and A.O. Aina, "Stability-improved perovskite solar cells through 4-tertbutylpyridine surface-passivated perovskite layer fabricated in ambient air", Opt. Mater. Vol. 112, pp. 110753, 2021, https://doi.org/10.1016/j.optmat.2020.110753.

[3] S.C. Ezike, "Stability Improvement of Perovskite Thin Films Through Surface Modifications for Perovskite Solar Cells Fabrication", Thesis, Kwara State University, 2018.

[4] A.N. Ossai, A.B. Alabi, S.C. Ezike, and A.O. Aina, "Zinc oxide-based dye-sensitized solar cells using natural and synthetic sensitizers", CRGSC, Vol. 3, pp.100043, 2021, https://doi.org/10.1016/j.crgsc.2020.100043.

[5] A.N. Ossai, S.C. Ezike, and A.B. Dikko, "Bio-synthesis of zinc oxide nanoparticles from bitter leaf (vernonia amygdalina) extract for dye-sensitized solar cell fabrication", J. Mater. Environ. Sci. 11, pp. 444-451, 2020.

[6] A.R. Jordehi, "Parameter estimation of solar photovoltaic (PV) cells: A review", Renwe. Sustain. Energy rev. Vol. 61, pp.354-371, 2016, https://doi.org/10.1016/j.rser.2016.03.049.

[7] W. De Soto, S. Klein, and W. Beckman, "Improvement and validation of a model for photovoltaic array performance", Sol. Energy Vol. 80, pp. 78-88, 2006, https://doi.org/10.1016/j.solener.2005.06.010.

[8] A. Laudani, F. Riganti-Fulgenei, and A. Salvini, "Identification of the one-diode model for photovoltaic modules from datasheet values", Solr energy, Vol. 108 pp. 432-446, 2014, https://doi.org/10.1016/j.solener.2014.07.024.

[9] A. Luadani, F. Mancill-David, F. Riganti-Fulgenei, and A. Salvini, "Reduced form of the photovoltaic five-parameter model for efficient computation of parameters", Sol. Enrgy Vol. 97, pp. 122-127, 2013, http://dx.doi.org/10.1016/j.solener.2013.07.031.

[10] A.H. ALQahtani, "A simplified and accurate photovoltaic module parameters extraction approach using matlab", In proceedings of the 2012 IEEE International Symposium on Industrial Electronics, Hangzhou, China, 28-30, 2012, pp. 1748-1753, https://doi.org/10.1109/ISIE.2012.6237355.

[11] S. Lineykin, M. Averbukh, Kuperman, "An improved approach to extract the single-diode equivalent circuit parameters of a photovoltaic cell/panel", Renew. Sustain. Energy Rev., Vol. 30, pp. 282-289, 2014, https://doi.org/10.1016/j.rser.2013.10.015.

[12] M. Villalva, J. Gazoli, and E. Filho, "Comprehensive approach to modeling and simulation of photovoltaic arrays", IEEE Trans. Power Electron. Vol. 24, pp. 1198-1208, 2009, https://doi.org/10.1109/TPEL.2009.2013862.

[13] R. Chenni, M. Makhlouf, T. Kerbache, and A. Bouzid, "A detailed modeling method for photovoltaic cells", Energy, Vol. 32, pp. 1724-1730, 2007, https://doi.org/10.1016/j.energy.2006.12.006.

[14] C. Carrero, D. Ramfrez, J. Rodriguez, and C. Platero, "Accurate and fast convergence method for parameter estimation of PV generators based on three main points of the curve", Renew. Energy, Vol. 36, pp. 2972-2977, 2011, https://doi.org/10.1016/j.renene.2011.04.001.

[15] Y.A. Mahmoud, W. Xiao, and H.H. Zeineldin, "A parameterization approach for enhancing PV model accuracy", IEEE. Trans. Ind. Electron Vol. 60, pp. 5708-5716, 2013, https://doi.org/10.1109/TIE.2012.2230606.

[16] S. Cannizaro, M.C. Di Piazza, M. Luna, and G. Vitale, "Generalized classification of PV modules by simplified single-diode models", In proceedings of the 2014 IEEE 23rd int. Symposium on industrial Electronics (ISIE), Istanbul, Turkey, 1-4 June pp. 2266-2273, 2014, https://doi.org/10.1109/ISIE.2014.6864971.

[17] J. Accarino, G. Petrone, C.A. Ramos-paja, and G. Spagnuola, "Symbolic algebra for the calculation of the series and parallel resistances in PV module model", In proceedings of the 2013 int. conference on clean electrical power (ICCEP), Alghero, Italy, 11-13 June (2013) 62-66, https://doi.org/10.1109/ICCEP.2013.6586967.

[18] I. Nassar-eddine, A. Obbadi, Y. Errami, A. El fajri, and M. Agunaou, "Parameter estimation of photovoltaic modules using iterativemethod and the Lambert W function: a comparative study", Energy convers. Manag., Vol. 119, pp. 37-48, 2016, https://doi.org/10.1016/j.enconman.2016.04.030.

[19] D. Sera, R. Teodorescu, and P. Rodriguez, "Photovoltaic module diagnostics by series resistance monitoring and temperature and rated power estimatimation", In the proceedings of 2008 34th annual conference of IEEE Industrial Electronics, Orland, FL, USA, 10-13 November, pp. 2195-2199, 2008, https://doi.org/10.1109/IECON.2008.4758297.

[20] F. Khan, S.H. Back, Y. Park, and J.H. Kim, "Extraction of diode parameters of silicon solar ccells under high illumination conditions", Energy convers. Manag., Vol. 76, pp. 421-429, 2013, https://doi.org/10.1016/j.enconman.2013.07.054.

[21] E.I. Batzelis, and S.A. Papathanassiou, "A method for the analytical extraction of the single-diode PV model parameters", IEEE Trans. Sustain. Energy, Vol. 7, pp. 504-512, 2016, http://dx.doi.org/10.1109/TSTE.2015.2503435.

[22] M. Hejri, H. Mokhtari, M.R. Azizian, and L. Soder, "An analytical-numerical approach for parameter determination of a five-parameter single-diode model of photovoltaic cells and modules", Int. J. Sustain. Energy, Vol. 396-410, 2016, https://doi.org/10.1080/14786451.2013.863886.

[23] A. Senturk, and R. Eke, "A new method to simulate photovoltaic performance of crystalline silicon photovoltaic modules based on datasheet values", Renew. Energy, Vol. 103, pp. 58-69, 2017, https://doi.org/10.1016/j.renene.2016.11.025.

[24] A. Murtaza, U. Munir, M. Chiaberge, P. Di Leo, and F. Spertino, "Variable parameters for a single exponential model of photovoltaic modules in crystalline silicon", Energies, Vol. 11, p. 2138, 2018, https://doi.org/10.3390/en11082138.

[25] H. Ibrahim, and N. Anani, "Evaluation of analytical merthods for parameter extraction of PV modules", Energy procedia, Vol. 134, pp. 69-78, 2017, https://doi.org/10.1016/j.egypro.2017.09.601.

[26] G. Xiong, J. Zhang, X. Yuan, D. Shi, Y. He, and G. Yao, "Parameter extraction of solar photovoltaic modelsby means of a hybrid differential evolution with whale optimization algorithm", Sol. Energy, Vol. 176, pp. 742-761, 2018, https://doi.org/10.1016/j.solener.2018.10.050.

[27] F.J. Toldo, J.M. Blanes, and V. Galiano, "Two-step linear least-squares method for photovoltaic sinle diode model parameter extraction", IEEE Trans. Ind.

Electron, Vol. 65, pp. 6301-6308, 2018, https://doi.org/10.1109/TIE.2018.2793216.

[28] G. Ciulla, V. Lo Brano, V. Di Dio, and G.A. Cipriani, "Comparison of different one-diode models for the representation of I-V characteristic of a PV cell", Renew. Sustain, Energy Rev., Vol. 32, pp. 684-696, 2014, https://doi.org/10.1016/j.rser.2014.01.027.

[29] A. Babangida, J.B. Yerima, A.D. Ahmed, and S.C. Ezike, "Strategy to select and grade efficient dyes for enhanced phot-absorption", African scientific reports, Vol. 1, pp. 16-22, 2022.

[30] J.B. Yerima, A. Babangida, S.C. Ezike, W. Dunama, and A.D. Ahmed, Matrix method of determining optical energy bandgap of natural dye extracts", J. Appl. Sci. Environ. Manage., Vol. 26, pp. 943-948, 2022, https://doi.org/10.4314/jasem.v26i5.22.

[31] E.I. Batzelis, "Simple PV performance equations theoretically well-founded on the single-diode model", IEEE J. Photovolt., Vol. 7, pp. 1400-1409, 2017, https://doi.org/10.1109/JPHOTOV.2017.2711431.

[32] J. Merten, J. Asensi, C. Voz, A. Shah, R. Platz, and J. Andreu, "Improved equivalent circuit and analytical model for amorphous silicon solar cells and module", IEEE Trans. Electron devices, Vol. 45, pp. 423-429, 1998, https://doi.org/10.1109/16.658676.

[33] R. Alayi, H. Harasii, H. Pourderogar, "Modeling and optimization of photovoltaic cells with GA algorithm", Journal of Robotics and Control (JRC), Vol. 2, pp. 35-41, 2021, https://doi.org/10.18196/jrc.2149.

[34] R. Alayi, M. Mohkam, S. R. Seyednouri, M. H. Ahmadi, and M. Sharifpur, "Energy/Economic Analysis and Optimization of On-Grid Photovoltaic System Using CPSO Algorithm", Sustainability, Vol. 13, pp. 12420, 2021, https://doi.org/10.3390/su132212420.

[35] A. Abbasi, R. Gammoudi, M. Ali Dami, O. Hasnaoui, and M. Jemli, "An improved single-diode model parameters extraction at different operating conditions with a view to modeling a photovoltaic generator: A comparative study", Sol. Energy, Vol. 155, pp. 478-489, 2017, https://doi.org/10.1016/j.solener.2017.06.057.

[36] A.N. Celik and N. Acikgoz, "Modeling and experimental verification of the operating current of mono-crystalline photovoltaic modules using four-and five- parameter models", Appl. Energy, Vol. 84, pp. 1-15, 2007, https://doi.org/10.1016/j.apenergy.2006.04.007.

[37] M. Hejri, H. Mokhtari, M.R. Azizianb, M. Ghandhari, and L. Soder, "On the parameter extraction of a five parameter double-diode model of photovoltaic cells and modules", IEEE J. Photovolt, Vol. 4 pp. 915-923, 2014, https://doi.org/10.1109/JPHOTOV.2014.2307161.

[38] R. Alayi, M. Jahangiri, J.W.G. Guerrero, R. Akhmadeev, R.A. Shichiyakh, S.A. Zanghaneh, "Modelling and reviewing the reliability and multi-objective optimization of wind-turbine system and photovoltaic panel with intelligent algorithms", Clean Energy, Vol. 5, pp. 713-730, 2021, https://doi.org/10.1093/ce/zkab041.

[39] H. Pourderogar, H. Harasi, R. Alayi, S. H. Delbari, M. Sadeghzadeh, and A. Javaherbakhsh, "Modeling and Technical Analysis of Solar Tracking System to Find Optimal Angle for Maximum Power Generation using MOPSO Algorithm", Renewable Energy Research and Application, Vol. 1, pp. 211-222, 2019, https://doi.org/10.22044/rera.2020.9497.1027.

[40] S.C. Ezike, C.N. Hyelnasinyi, M. A. Salawu, J.F. Wansah, A.N. Ossai, and N.N. Agu, "Synergestic effect of chlorophyll and anthocyanin Co-sensitizers in TiO2-based dye-sensitized solar cells", Surfaces and Interfaces, Vol. 22, pp. 100882, 2021, https://doi.org/10.1016/j.surfin.2020.100882.

[41] A. N Ossai, S. C Ezike, P. Timtere, and A. D. Ahmed, "Enhanced photovoltaic performance of dye-sensitized solar cells-based Carica papaya leaf and black cherry fruit co-sensitizers", Chemical Physics Impact,Vol. 2, pp. 100024, 2021, https://doi.org/10.1016/j.chphi.2021.100024.

[42] U.I Ndeze, J. Aidan, S.C Ezike, and J.F Wansah, "Comparative performances of nature-based dyes extracted from Baobab and Shea leaves photo-sensitizers for dye-sensitized solar cells (DSSCs)", Current Research in Green and Sustainable Chemistry, Vol. 4, pp. 100105, 2021, https://doi.org/10.1016/j.crgsc.2021.100105.

[43] M.A. Salawu, A. A Ayobami, A. Adebisi, S.C. Ezike, Y. O. Saheed, and A. B. Alabi, "Characterization of eosin red and hibiscus sabdariffa-based dye-sensitized solar cells", Optical Materials, Vol. 127, pp. 112177, 2022, https://doi.org/10.1016/j.optmat.2022.112177.

[44] H.P Wante, J. Aidan, and S.C Ezike, "Efficient dye-sensitized solar cells (DSSCs) through atmospheric pressure plasma treatment of photoanode surface", Current Research in Green and Sustainable Chemistry, Vol. 4, pp. 100218, 2021, https://doi.org/10.1016/j.crgsc.2021.100218.

[45] S.C. Ezike, G.M.Z. Kana, and A.O. Aina, "Progress and prospect on stability of perovskite photovoltaics", Journal of Modern Materials, Vol. 4, pp. 16-30, 2017, https://doi.org/10.21467/jmm.4.1.16-30.

[46] A.M. Tayeb, A.A.A. Solyman, M. Hassan, and T. M. Abu el-Ella, "Modeling and simulation of dye-sensitized solar cell: Model verification for different semiconductors and dyes", Alexandria Engineering Journal, Vol. 61, pp. 9249-9260, 2022.

[47] S.A. Badawy, E. Abdel-latif, A.A. Fadda, M.R. Elmorsy, "Synthesis of innovative triphenylamine-

functionalized organic photosynthesizers outperformed the benchmark dye N719 for high-efficient dye-sensitized solar cells", Sci Rep, Vol. 12, pp. 12885, 2022.

[48] R. Venkateswari and N. Rajasekar, "Reiview on power estimation techniques of solar photovoltaic system", International Transaction on Electrical Energy System, Vol. 31, pp. e13113, 2021, https://doi.org/10.1002/2050-7038.13113.

[49] M.D. Abbot, T. Trupke, H.P. Hartmann, R. Gupta, and O. Breitenstein, "Laser isolation of shunted regions in industrial solar cells", Progress in Photovoltaics: Research and Applications, Vol. 15, pp. 613-620, 2007